Biosensors and Bioelectronics 40 (2013) 401–406

Contents lists available at SciVerse ScienceDirect

Biosensors and Bioelectronics

journal homepage: www.elsevier.com/locate/bios

Bioengineered olfactory sensory neuron-based biosensor for specific odorant detection

Liping Du [a], Chunsheng Wu [a], He Peng [b], Luhang Zhao [b], Liquan Huang [c], Ping Wang [a,*]

[a] Biosensor National Special Laboratory, Key Laboratory for Biomedical Engineering of Ministry of Education, Department of Biomedical Engineering, Zhejiang University, Hangzhou 310027, China
[b] Department of Biochemistry and Genetics, School of Medicine, Zhejiang University, Hangzhou 310058, China
[c] Monell Chemical Senses Center, 3500 Market Street, Philadelphia, Pennsylvania 19104, USA

ARTICLE INFO

Available online 12 September 2012

Keywords:
Bioengineered olfactory sensory neurons
Light addressable potentiometric sensor (LAPS)
Cell-based biosensor
Odorant detection

ABSTRACT

It is highly desirable to obtain functional cells with specific olfactory receptors (ORs) for the development of cell-based biosensors towards odorant detection. In this study, we explored the feasibility of bioengineered primary olfactory sensory neurons (OSNs) as sensing elements of biomimetic olfactory-based biosensors, in which light addressable potentiometric sensor (LAPS) was used to monitor bioengineered OSNs membrane potential responses to odorant molecules. An olfactory receptor of *C. elegances*, ODR-10, as a model receptor, was expressed on the plasma membrane of OSNs by transient transfection. The response profile of bioengineered OSNs to odorant molecules was investigated by analyzing extracellular potential firings features in frequency and time domains. The results indicated that bioengineered OSNs can specifically respond to diacetyl, the natural ligand of ODR-10. In addition, bioengineered OSNs showed different temporal firing patterns in responding to different concentrations of diacetyl. All the results demonstrate that bioengineered OSNs are useful and promising to serve as novel sensing elements of biosensors for specific odorant molecule detection. It is suggested that bioengineering techniques could provide novel approaches for preparing sensitive elements as well as promoting the development of practical applicable olfactory-based biosensors.

© 2012 Elsevier B.V. All rights reserved.

1. Introduction

The mammal olfactory system has an excellent capacity in recognizing and discriminating various odorants. The fundamental sensing elements are olfactory sensory neurons (OSNs), in which olfactory receptors (ORs) and related intracellular signal pathways are crucial to the function of odorant detection. The discovery of gene family encoding vertebrate ORs (Buck and Axel, 1991) has paved the way for the research of olfactory system, such as olfactory molecular sensing mechanisms, signal transduction pathways, and olfactory information encoding and decoding. In the mammal olfactory system, ORs, located on the plasma membrane of OSNs, can interact with odorants specifically. With the aid of related intracellular signal transduction pathways, the odorant chemical information is transformed into the potential firing of OSNs (Breer, 2003). OSNs can encode the chemical information at the population level, and the peripheral olfactory signal encoding can transmit the olfactory information to the central neural system (Hoare et al., 2011). The ability of preliminary information encoding is also a crucial factor of the powerful odorant discrimination ability, which contributes much to the complex odorant discrimination. All these characteristics make OSNs ideal candidates to serve as sensing elements for the development of biomimetic olfactory-based biosensors towards specific odorant detection.

In recent years, biomimetic olfactory-based biosensor has become a promising research field and great effort is put into the development of novel highly sensitive olfactory biosensors using various biological olfactory components as sensing elements (Glatz and Bailey-Hill, 2011). The olfactory tissues (Chen et al., 2011; Liu et al., 2010), OSNs (Liu et al., 2006; Wu et al., 2009), and ORs (Kim et al., 2009; Ko and Park, 2005; Misawa et al., 2010; Sankaran et al., 2011a, 2011b; Sung et al., 2006; Wu et al., 2011b) have been employed as the sensing elements of olfactory biosensors. In addition, olfactory coding mechanisms are also applied in the development of olfactory biosensors for improving the performance (Beccherelli et al., 2010). Among those biological olfactory components, ORs are the most fundamental odorant detection elements. The specific interaction between ORs and odorants is the common basis of biomimetic olfactory-based biosensors. Several groups have developed the highly sensitive biosensors by directly detecting the interaction of ORs and

* Corresponding author. Tel./fax: +86 571 87952832.
E-mail address: cnpwang@zju.edu.cn (P. Wang).

0956-5663/$ - see front matter © 2012 Elsevier B.V. All rights reserved.
http://dx.doi.org/10.1016/j.bios.2012.08.035

odorants via piezoelectric transducers (Ko and Park, 2005; Sankaran et al., 2011a, 2011b; Sung et al., 2006; Wu et al., 2011b). But the performance of ORs-based biosensors is limited due to the difficulties in the production of highly purified ORs. On the other hand, primary OSNs and olfactory epithelium are more promising to improve the performance of biosensors in complex environment due to their distinct signal response modes and innate encoding ability (Chen et al., 2011; Liu et al., 2006, 2010; Kim et al., 2012; Wu et al., 2009). However, it is too complicated to process the detected firing signals and discriminate the different responses of various odorants, owing to the unknown type of ORs in desired OSNs and the unrevealed olfactory encoding mechanisms (Quiroga and Panzeri, 2009). Therefore, it is highly desirable to obtain functional OSNs with specific ORs through a simplified approach in order to develop novel olfactory-based biosensors for specific odorant detection.

In this study, we proposed a novel bioengineered OSNs-based biosensor for odorant detection in order to explore the feasibility of using bioengineered primary OSNs as sensing elements, which combined the distinct features of ORs and OSNs. Primary OSNs were isolated from the rat olfactory epithelium and cultured on the surface of light addressable potentiometric sensor (LAPS) chip. Bioengineered OSNs were produced by expressing a model OR protein (an olfactory receptor of *C. elegances*, ODR-10) on the plasma membrane of primary OSNs through transient transfection. Bioengineered OSNs not only maintained the natural signal transduction components and innate coding mechanisms, but also bore specific type of ORs. By coupling the bioengineered ORNs with LAPS chip, the extracellular potential firings can be monitored by illuminating the desired single bioengineered OSN on LAPS surface. Several signal processing methods were employed to analyze the odorant-induced firing information. The distinct characteristics were investigated in frequency and time domains.

2. Experiments

2.1. LAPS chip and detection system

For LAPS chip fabrication, the upper side of N-type silicon wafer (500 μm thick, 10–15 Ω cm) is oxidized thermally at 1000 °C with a layer of 30 nm SiO_2. To enhance the sensitivity of LAPS, the silicon substrate is ground to 100 μm thick from the back side. Then aluminum is evaporated on the back side of silicon wafer to create an ohmic contact, which is used as the working electrode. The detection chamber is sealed onto the upside of LAPS chip. Platinum wire is used as the counter electrode and Ag/AgCl electrode as the reference electrode. Fig. 1(a) shows a photo of LAPS chip with a sealed detection chamber. Fig. 1(c) is the schematic diagram of LAPS detection system. The LAPS detection system is adopted from our previous reported work (Liu et al., 2006; Wu et al., 2009), which is a three-electrode system. By illuminating the focused laser (10 μm in diameter, 543.5 nm wavelength and 5 mW power) on the desired bioengineered OSN on LAPS surface, photocurrent fluctuation originated from extracellular potential changes can be detected by potentiostat (EG&G Princeton Applied Research, M273A) and recorded by lock-in amplifier (model SR830 DSP, Stanford Research Systems). The customized software of LABVIEW is used to collect, analyze, and store the experiment data.

2.2. Bioengineered OSN

Primary OSNs were prepared from the olfactory epithelium of 3-day-old Sprague-Dawley (SD) rats. The rat was decapitated and the nose was dissected. The entire intact olfactory epithelium was gently peeled away from the underlying bone. Then the olfactory epithelium was incubated with the enzyme solution of 0.25% trypsin (pH 7.4–7.8) at 37 °C for 20 min and transferred to mammalian Ringer's solution for blowing gently with pipette. Dissociated cells were subsequently filtered into the suspension of fresh Dulbecco's modified Eager's medium (DMEM) with 10% fetal bovine serum (FBS). Then the suspension was added into the detection chamber of LAPS. Cells were allowed to settle down and attach on the surface of LAPS chip at 37 °C under standard conditions of humidified air with 5% CO_2.

To build bioengineered OSNs, the expression plasmid *pEGFP-N1/rho-tag/odr-10* containing *odr-10* gene was constructed, in which enhanced green fluorescent protein (EGFP) was used to indicate the expression of ODR-10 on the cellular membrane. The detailed construction procedure was present in our previous paper (Wu et al., 2011a). Here the expression plasmid *pEGFP-N1/rho*-tag/*odr-10* was transiently transfected into primary OSNs on the LAPS chip and then specific OR (ODR-10) was expressed on the cellular membrane of OSNs. After 12 h transfection, the extracellular potential firings of bioengineered OSNs were recorded by LAPS chip at room temperature.

2.3. Odorants stimulation

Phosphate buffer solution (PBS) was used as negative control solution. Diacetyl, the natural ligand of ODR-10, was used as the stimulus in this study and diluted with PBS into 5 concentrations: 0.1 μM, 1 μM, 10 μM, 50 μM, and 100 μM. Isoamyl acetate and acetic acid were employed for the selectivity test, and diluted to 50 μM. At the beginning of recording, control solution was added into the detection chamber to record extracellular spontaneous potential firings. Then a certain concentration of odorant solution was introduced into the detection chamber to investigate the responses of bioengineered OSNs. After that the stimulus of odorant solution was removed by washing with fresh PBS. The minimum interval of odorant solution addition was 5 min. All recordings lasted 10 min and were carried out at room temperature (18–25 °C).

2.4. Data processing

The experiment data were collected by a 16-bit data collection card and data recording process was controlled by the software of LABVIEW. Sampling rate is 10 kHz. All the signal processing was performed using custom programs written in MATLAB software. The acquired raw data were firstly smoothed by the high-pass filter to remove the baseline drift. By fast Fourier transform (FFT), the power spectrum was obtained and the characteristics in the frequency domain were investigated. To analyze firing properties in the time domain, we employed peak value extraction method to obtain the firing spikes. The spontaneous firing signals without stimulus were taken as the control signal. The mean value '*D*' of the control signal was used to quantify the baseline noise. The spike detection was based on threshold method. The criterion of threshold selection was to get a relative low error spike detection rate and undetected rate. The optimized threshold was set to 2.5**D* and spikes with amplitude above threshold were extracted. On the basis of the spikes above the threshold, the later temporal firing responses were quantified mainly by three methods, namely the mean firing rate, peri-stimulus time histograms (PSTHs) and interspike interval histograms (ISIHs). The mean firing rate was defined as the total number of firing spikes in 60 s. PSTHs were used to visualize the firing rate in different time after stimulus. A period of observation time T was divided into N bins with 1 s bin size. The number of spikes in each successive 1 s bin represented the height of PSTHs bar histogram. ISIHs were the distribution of the intervals between spikes and could reflect the patterns of spike activity in one aspect.

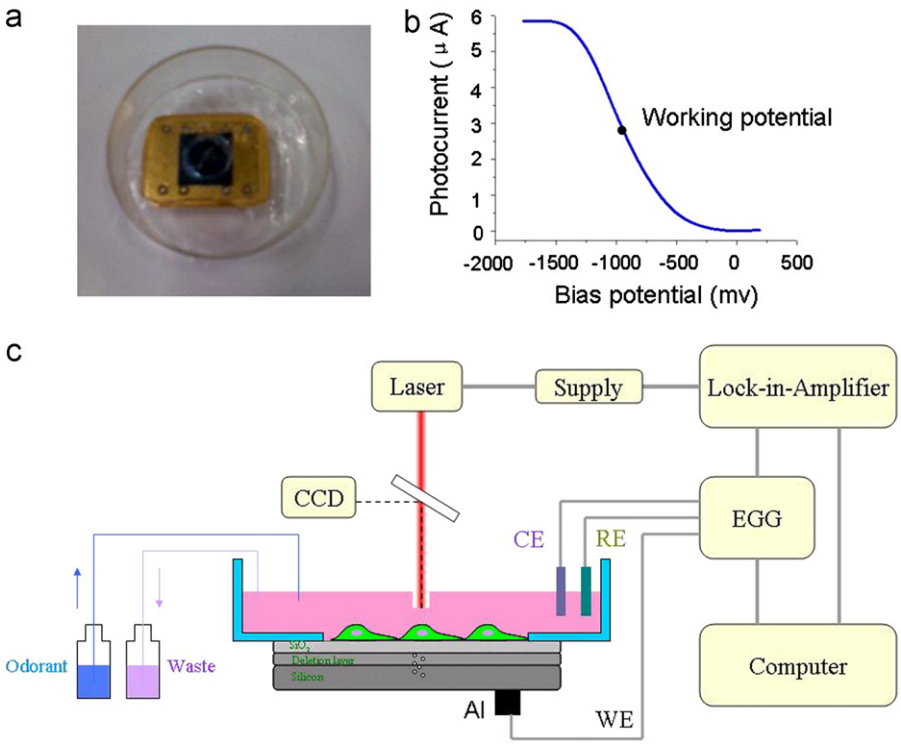

Fig. 1. (a) A photo of LAPS chip with a sealed detection chamber. (b) The characteristic curve of LAPS (photocurrent vs. bias potential). (c) A schematic diagram of LAPS detection system.

3. Results and discussion

3.1. OSNs cell culture on LAPS chip

The olfactory epithelium mainly contains three types of cells, namely ciliated olfactory sensory neurons (OSNs), supporting cells, and progenitor/stem cells (Munger et al., 2009). OSNs are the primary sensing cells and they are bipolar neurons with a single dendrite. The results demonstrated that bioengineered OSNs cultured on the LAPS sensor still maintained their special neural morphology. Fig. 2(a) showed the typical shape of OSNs cultured on LAPS surface, which was a kind of typical spindle shapes. To visualize the expression of ODR-10 in bioengineered OSNs, EGFP was co-expressed with ODR-10 to serve as an expression reporter. The sub-cellular distribution of EGFP can report the location of ODR-10. Fig. 2(b) was a fluorescence photo of bioengineered OSNs, it's shown that fluorescent can be observed in most OSNs and was mainly distributed on the plasma membrane. This indicated that ODR-10 proteins were efficiently expressed on the OSNs and the bioengineered OSNs were constructed successfully. In addition, the expressed ODR-10 was mainly distributed on the plasma membrane of OSNs, which can facilitate the specific interactions between expressed ORs and odorant molecules.

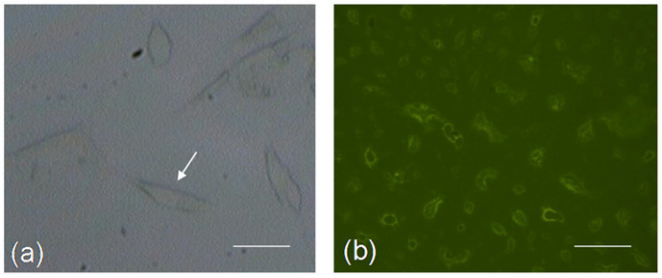

Fig. 2. Images of bioengineered OSNs on the LAPS sensor. (a) Bioengineered OSNs under the light field, bar is 10 μm. (b) Bioengineered OSNs under the fluorescence field, bar is 30 μm.

3.2. Extracellular potential firings of bioengineered OSNs

LAPS is a type of field effect device, which is suitable for the surface potential detection. It typically consists of an electrolyte–insulator [SiO_2]–semiconductor [Si] structure. The detailed detection principle of LAPS chip has been discussed elsewhere (Liu et al., 2006). When the LAPS chip is illuminated by light of a certain wavelength, electron–hole pairs will be generated in the semiconductor layer. However, electron–hole pairs will recombine quickly and the periphery circuit cannot detect the current. If the semiconductor is set at a bias voltage, a depletion layer will be formed and electron–hole pairs will be separated by the electrical field. The width of the depletion layer is a function of the local value of the surface potential, which can be read out with alternating photocurrents. Fig. 1(b) showed a typical photocurrent vs. bias potential characteristic curve of LAPS and the corresponding potential value in the greatest slope was selected as the working potential point. Then the extracellular potential changes of OSNs can be read out by recording the photocurrent fluctuations. By moving the modulated light pointer, the surface potential of every spot on the LAPS can be read out. Its extraordinary addressable performance made it suitable for detecting single cells in cell population.

Fig. 3(a) showed typical extracellular potential firing signals of bioengineered OSNs. The noise was about 20 μV. The upper panel of Fig. 3(a) was a spontaneous firing signal under the control solution without any odorant solution, from which sparse spikes can be observed. However, more spikes were elicited by 10 μM diacetyl, as shown in the lower panel of Fig. 3(a). The intuitive difference in the firing rate can be observed at first glance. To investigate the characteristic differences in the frequency domain, we performed fast Fourier transform (FFT) analysis and

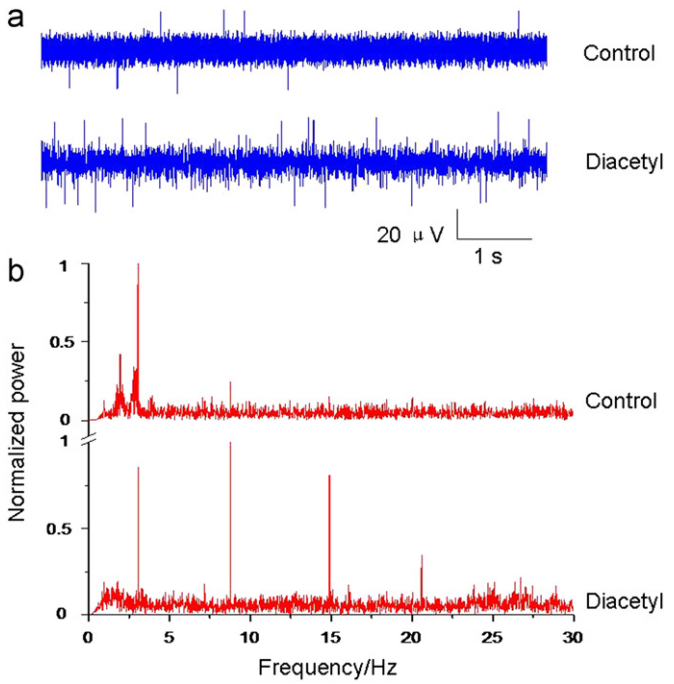

Fig. 3. The potential firings and the corresponding power spectra. (a) Spontaneous (upper) and 10 μM diacetyl-stimulated (lower) signals. (b) Normalized power spectra corresponding to spontaneous (upper) and 10 μM diacetyl-stimulated (lower) signals.

obtained the normalized power spectra in the low frequency band of 0–30 Hz, as shown in Fig. 3(b). The upper one corresponded to the spontaneous signal under the control solution and the lower one was the power spectrum of 10 μM diacetyl-stimulated firing signal. In the power spectrum of spontaneous firing, the dominating frequency component was 3 Hz, and another two minor frequency peaks located at 2.4 Hz and 8.4 Hz. This was consistent with the spontaneous characteristics observed from the olfactory epithelium, in which 3 Hz was also the major frequency peak (Liu et al., 2010). Therefore the other two minor frequency peaks could be thought to be the distinct firing characteristics of bioengineered OSNs. Compared to the spontaneous state, the diacetyl-induced firing had different frequency components, in which three major frequency peaks were at 3 Hz, 8.4 Hz, and 15 Hz, respectively, and there was also a minor peak at 21 Hz. Two common frequency components of two states were 3 Hz and 8.4 Hz, but their proportions in the two spectra differ significantly. The power of dominating component in the control group (3 Hz) decreased in the diacetyl-induced group, while the minor component of control group (8.4 Hz) became the most dominating component in the odorant-induced signals. Additionally, another two frequency components (15 Hz and 21 Hz) were the distinct frequency characteristics of diacetyl-induced signals. We tested different concentrations of diacetyl ranging from 0.1 μM to 100 μM. The results demonstrated that the feature of frequency spectrum in each concentration was similar to that of 10 μM diacetyl. But the energy of frequency spectrum in each concentration was different, which increased with the odorant concentration increment. All these results demonstrated that there were common as well as obvious different frequency characteristics between the spontaneous state and odorant-induced states. It can be conferred that the spontaneous firing of bioengineered OSNs may be the important basis of olfaction signal encoding and the odorant information could be encoded in the characteristics of the frequency domain.

3.3. Temporal characteristics analysis

In the natural world, different kinds of odorants, as well as different concentrations of one odorant, can be discriminated by biological olfactory systems. Even the same odorant can induce different smell responses at different concentrations. For example, an odorant has a pleasant and attractive smell at low concentrations, but becomes putrid and repulsive when concentrated. Behavioral and genetic investigation have found the proof that distinct encoding abilities of OSNs function well in discriminating different concentrations of odorants (Yoshida et al., 2012).

The responses of bioengineered OSNs to different concentrations of odorant solutions were shown in Fig. 4, which were evaluated preliminarily by the mean firing rate. It can be found that the firing of bioengineered OSNs increased with the increasing concentrations of diacetyl ranging from 0.1 μM to 100 μM, which was also consistent to that observed in the frequency domain. But the responses were not in a strict dose-dependent way, which overlapped a bit in some different concentrations. It's probably because the mean firing rate could not fully depict the complex mechanisms of bioengineered OSNs responding to odorant molecules. Especially in the range of lower concentrations, the information between different concentrations cannot be effectively discriminated. From the concentration–response curve, an interesting phenomenon can be found that there was a steep transition from 10 μM to 50 μM. This may attribute to the different encoding mechanism of bioengineered OSNs to the low/high concentration of odorant solutions, which would be further analyzed later.

To test the specificity of bioengineered OSNs, isoamyl acetate (IA) and acetic acid (AA) were used as control odorant solutions, whose concentration was 50 μM. The response to each odorant solution was normalized by that to diacetyl. The normalized result was shown in the inset of Fig. 4. It is demonstrated that the response to diacetyl was significantly higher than those to isoamyl acetate and acetic acid. Moreover, the mixture of isoamyl acetate and acetic acid were also tested. Comparing the responses to mixture solutions with diacetyl and without diacetyl, we found that bioengineered OSNs could still respond to mixture odorants

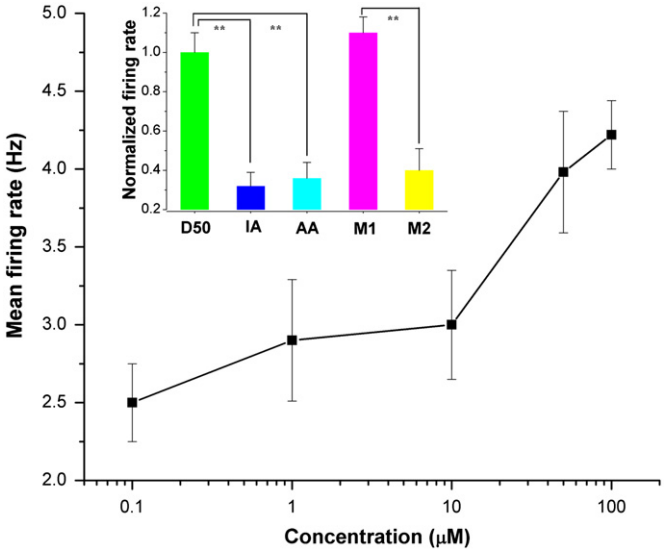

Fig. 4. The concentration–response curve to varying concentrations of diacetyl. The inset figure is the result of the normalized specificity test. D50 represents 50 μM diacetyl; IA, isoamyl acetate; AA, acetic acid; M1, the mixture of diacetyl, isoamyl acetate, and acetic acid; M2, the mixture of isoamyl acetate and acetic acid. The concentration of each odorant is 50 μM. Data are presented as mean ± SD (standard deviation). Each data points are obtained by 5 times of experiments. Significant differences are indicated by ** ($P < 0.01$) using Student's t-test.

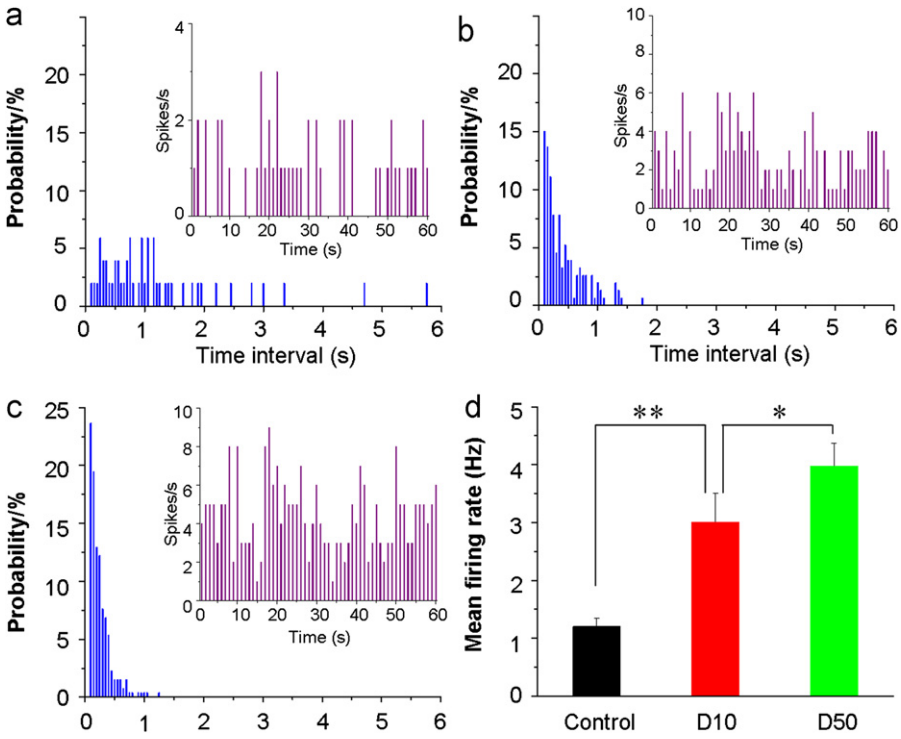

Fig. 5. The temporal response characteristics of the bioengineered OSN-based biosensor are investigated by PSTHs (purple) and ISIs (blue). (a) The spontaneous firing state as a control group. (b) and (c) are the results of 10 μM and 50 μM diacetyl, respectively. (d) Mean firing rate statistics of three states, namely control group, 10 μM diacetyl (D10) and 50 μM diacetyl (D50) stimulated firings. Data are presented as mean ± SD (standard deviation). Each data points are obtained by 5 times of experiments. Significant differences are indicated by (**$P < 0.01$) and (*$P < 0.05$) using Student's *t*-test. (For interpretation of the references to color in this figure legend, the reader is referred to the web version of this article.)

with diacetyl specifically. It is inferred that bioengineered OSNs with ORs (ODR-10) had good specificity to the natural ligand of ODR-10.

To explore the steep transition in the concentration–response curve, 10 μM was labeled as the low concentration of diacetyl, and 50 μM as the high concentration. The temporal firing characteristics of bioengineered OSNs were further analyzed by two methods, namely peri-stimulus time histograms (PSTHs) and interspike interval histograms (ISIHs). All these methods were based on the analysis of spikes above the defined threshold. PSTHs reflected the distribution of spikes over time after stimulus, while ISIHs was frequency distribution of the intervals between all the successive discriminated spikes to examine changes in inter-spike interval over time.

Fig. 5(a) was the PSTHs and ISIHs of spontaneous firing signal without any stimulus, which was used as a control group. The ISIHs result demonstrated that spike intervals scatter in the range of 0–6 s and mostly distributed in the range of 0–3 s (> 95%). The mean firing rate in one second was less than 2 spikes/s and there was no spikes firing in some time ranges (observed from the inset figure, PSTHs). It meant that bioengineered OSNs had random sparse electrical activities in the spontaneous state. After the stimulation of 10 μM diacetyl, the firing rate of OSNs became obviously higher than that of spontaneous state. The firing activities also showed smaller spike intervals mainly in the range of 0–2 s, as presented in Fig. 5(b). When stimulated by 50 μM diacetyl, bioengineered OSNs displayed another different temporal firing mode as shown in Fig. 5(c). There were intensive firing activities in almost every second. The ISIH result demonstrated that majority of spike intervals were distributed in the range of 0–1 s. Compared to the control group, the odorant-induced firing activities became more intensive with the increase of odorant concentration. By calculating the mean firing rate in one minute, the same conclusion can also be obtained, as shown in Fig. 5(d). The mean firing rates of control group, 10 μM diacetyl (D10), and 50 μM diacetyl (D50) are 1.2 ± 0.15 ($n=5$), 3 ± 0.5 Hz ($n=5$), and 3.98 ± 0.39 Hz ($n=5$), respectively. Student's *t*-test was performed to analysis the significant difference between different groups. The results demonstrated that control group and 10 μM diacetyl group had very significant difference ($P < 0.001$), and the difference between 10 μM diacetyl and 50 μM diacetyl groups was also significant ($P < 0.005$).

As for the reproducibility, multiple biosensors were tested under the same condition. The results indicated that the reproducibility of these biosensors is limited (data not shown). It may be greatly due to the difference in the expression efficiency of ORs and bioengineered OSNs stability when attached to the surface of LAPS chip. A significant amount of additional work would be required in the standard fabrication of this biosensor to improve the reproducibility, which may include the improvement on the expression efficiency of ORs in OSNs and LAPS surface modification.

All the results from bioengineered OSNs-based LAPS biosensor indicated that the stimulus of odorant solutions could be encoded by the extracellular firing signals of bioengineered OSNs. The low/high concentration of odorant solution can be discriminated by temporal firing features. The biological intelligence of OSNs made bioengineered OSNs suitable sensitive materials of biosensors for odorant molecule detection and discrimination.

4. Conclusion and outlook

In this study, a bioengineered OSN-based LAPS biosensor was well developed for specific odorant molecule detection. The detection of diacetyl, the natural ligand of expressed OR (ODR-10), was achieved by analyzing the extracellular firing characteristics of the bioengineered OSNs in the frequency and time domains. The preliminary results demonstrated that this biosensor can specifically respond to diacetyl ranging from 0.1 μM to 100 μM. In addition, the specific firing patterns were also observed under low/high concentrations.

All the results demonstrate the bioengineered OSNs are suitable to serve as a new kind of sensitive elements for the development of olfactory-based biosensors for the specific detection of odorant molecules.

This is a proof-of-concept study on bioengineered OSNs-based biosensor. However, the proposed biosensor still suffers greatly from the limited reproducibility and sensitivity. It requires great effort to achieve the standard fabrication of biosensors for high sensitivity measurements and reproducibility to be suitable for practical applications. Data mining techniques may provide novel solutions for the signal processing to reveal the innate dose-dependent relationship, which could improve the performance of bioengineered OSNs-based biosensor by enhancing the ability of information discrimination and achieving the lower detection limit.

On the basis of proposed bioengineered OSNs-based biosensor, it was possible that bioengineered OSNs with different types of ORs could be cultured on the LAPS to form the distinct olfactory neuronal network for the detection of different odorants simultaneously. By combining signal processing techniques and olfactory decoding theories, the olfactory biosensor has great potential to detect and discriminate odorants in the complex environment for many applications, including environmental monitoring, food safety, and medical diagnosis. For example, this bioengineered OSNs-based biosensor could be further developed into an electronic nose for the non-invasive detection of biomarkers (i.e. volatile organic compounds, VOCs) in breath air of patients with lung diseases, which could provide helpful information for the early clinical diagnosis and therapy of specific lung diseases. In addition, this bioengineered OSN-based biosensor could also be used as a valuable platform for the research of olfactory extracellular electrophysiology, olfactory signal transduction mechanisms, and olfactory encoding patterns in a non-invasive manner.

Acknowledgments

This work was supported by the grants from the National Natural Science Foundation of China (Grant nos. 30970765, 31000448, 312280013), the China Postdoctoral Science Foundation (Grant no. 201104734) and the Key Project of Zhejiang Province (Grant no. 2010C14006). We thank Professor Cornelia I. Bargmann from Laboratory of Neural Circuits and Behavior, Howard Hughes Medical Institute, The Rockefeller University for providing cDNA of *odr-10*.

References

Beccherelli, R., Zampetti, E., Pantalei, S., Bernabei, M., Persaud, K.C., 2010. Sensors and Actuators B 146, 446–452.
Breer, H., 2003. Analytical and Bioanalytical Chemistry 377, 427–433.
Buck, L., Axel, R., 1991. Cell 65, 175–187.
Chen, Q.M., Xiao, L.D., Liu, Q.J., Ling, S.C., Yin, Y.F., Dong, Q., Wang, P., 2011. Biosensors and Bioelectronics 26, 3313–3319.
Glatz, R., Bailey-Hill, K., 2011. Progress in Neurobiology 93, 270–296.
Hoare, D.J., Humble, J., Jin, D., Gilding, N., Petersen, R., Cobb, M., McCrohan, C., 2011. PLoS One 6.
Kim, H., Kim, S.Y., Nam, S., Ronnett, G.V., Han, H.S., Moon, C., Kim, Y., 2012. Analyst 137, 2047–2053.
Kim, T.H., Lee, S.H., Lee, J., Song, H.S., Oh, E.H., Park, T.H., Hong, S., 2009. Advanced Materials 21, 91–94.
Ko, H.J., Park, T.H., 2005. Biosensors and Bioelectronics 20, 1327–1332.
Liu, Q.J., Cai, H., Xu, Y., Li, Y., Li, R., Wang, P., 2006. Biosensors and Bioelectronics 22, 318–322.
Liu, Q.J., Ye, W.W., Hu, N., Cai, H., Yu, H., Wang, P., 2010. Biosensors and Bioelectronics 26, 1672–1678.
Misawa, N., Mitsuno, H., Kanzaki, R., Takeuchi, S., 2010. Proceedings of the National Academy of Sciences of the United States of America 107, 15340–15344.
Munger, S.D., Leinders-Zufall, T., Zufall, F., 2009. Annual Review of Physiology 71, 115–140.
Quiroga, R.Q., Panzeri, S., 2009. Nature Reviews Neuroscience 10, 173–185.
Sankaran, S., Panigrahi, S., Mallik, S., 2011a. Biosensors and Bioelectronics 26, 3103–3109.
Sankaran, S., Panigrahi, S., Mallik, S., 2011b. Sensors and Actuators B 155, 8–18.
Sung, J.H., Ko, H.J., Park, T.H., 2006. Biosensors and Bioelectronics 21, 1981–1986.
Wu, C.S., Chen, P.H., Yu, H., Liu, Q.J., Zong, X.L., Cai, H., Wang, P., 2009. Biosensors and Bioelectronics 24, 1498–1502.
Wu, C.S., Du, L.P., Wang, D., Wang, L., Zhao, L.H., Wang, P., 2011a. Biochemical and Biophysical Research Communications 407, 18–22.
Wu, C.S., Du, L.P., Wang, D., Zhao, L.H., Wang, P., 2011b. Biosensors and Bioelectronics 31, 44–48.
Yoshida, K., Hirotsu, T., Tagawa, T., Oda, S., Wakabayashi, T., Iino, Y., Ishihara, T., 2012. Nature Communications 3, 739.